Purification of colloidal oil in water emulsions by cationic adsorbent prepared from recycled polyethylene waste

Sarah Hailan [a,b], Priya Ghosh [b], Patrik Sobolciak [b], Peter Kasak [b], Anton Popelka [b], Mabrouk Ouederni [c], Samer Adham [d], Mohamed Chehimi [e], Gordon McKay [a], Igor Krupa [b,f,*]

[a] Qatar Environment and Energy Research Institute, Hamad Bin Khalifa University, Qatar
[b] Center for Advanced Materials, Qatar University, P.O. Box 2713, Doha, Qatar
[c] QAPCO R&D – Qatar Petrochemical Company, P.O. Box 756, Doha, Qatar
[d] ConocoPhillips Global Water Sustainability Center, Qatar Science and Technology Park, P.O. Box 24750, Doha, Qatar
[e] ITODYS Lab, Université Paris Cité, CNRS (UMR 7086), 15 rue Jean-Antoine de Baïf, 75013 Paris, France
[f] Materials Science and Technology Graduate Program, College of Arts and Sciences, Qatar University, P.O. Box 2713 Doha, Qatar

ARTICLE INFO

ABSTRACT

This study deals with removing crude oil droplets from colloidal oil in water emulsions. The target was the development of efficient adsorbents for the tertiary treatment of industrial-produced water (PW). The novel adsorbent was designed from recycled low-density polyethylene (LDPE) powder grafted by the cationic polymer. The cationic polymer was synthesized directly on the LDPE surface by plasma-induced radical polymerization. A positively charged adsorbent was chosen due to the negative character of oily droplets to enhance separation efficiency in treating oil-water emulsions. The separation was performed in both batch and filtration modes. Absorption/adsorption uptake capacities showed a sigmoidal S-shape that was analyzed using the Sips model and compared with the newly developed empirical model. Both models showed a remarkable coincidence in the description of experimental data.

The separation efficiency of the novel adsorbent was also tested in a filtration mode mimicking a commonly used deep-bed filtration technology. The comparison of the separation efficiency for various sorbents indicated a supreme performance of novel adsorbent. This study demonstrates the potential of a relatively cheap, prepared commodity-based adsorbent for the purification of emulsified oily polluted water in both batch and filtration configurations. This study also contributes to the recycling of polyethylene waste because LDPE attracts meager interest in recycled LLDPE due to many obstacles to reusing LDPE waste for its reprocessing as packaging materials.

1. Introduction

Extraction and processing of oil and gas are associated with the consumption of vast volumes of water (Igunnu and Chen, 2014; Adham et al., 2018). It has been estimated that extraction of one barrel of oil requires from 3–4 barrels of water on average and around 10 barrels for aged sources Dores et al., 2012; Munirasu et al., 2016). The water resulting from this process is called produced water (PW) and consists of various saturated and unsaturated hydrocarbons, fatty acids, poly-aromatics, surfactants, inorganic salts (mainly NaCl), and other additives (Neff et al., 2011; Al-Ghouti et al., 2019). The complexity of PW involves an extensive range of dissolved and dispersed organic compounds, indicating the need for a series of sequential treatment processes. Primary, secondary, and tertiary treatments are applied depending on the concentration of organic compounds (oil & grease) (Industrial wastewater treatment technology, 2023; Pintor et al., 2016). Tertiary treatment reduces organics content in the effluents below ten ppm (Dickhout et al., 2017).

Current tertiary filtration technology mainly includes membrane filtration (Padaki et al., 2015; Tanudjaja et al., 2019; Al-Kaabi et al., 2019), activated carbon (Albatrni et al., 2019), synthetic resins (Rahman, 1992), and walnut shell filtration (Yin et al., 2021; Dąbrowski, 2001). Different separation techniques utilize other physical principles for separation. Whereas membrane filtration is based on the simple

---

separation of oil droplets according to their size, sand, crushed stone, activated carbon, and synthetic resins act based on an adsorption process, and the critical mechanism for deep bed filtration using wall nutshell media involves coalescence accomplished by adsorption. Adsorption is a relatively simple but efficient method commonly used for water purification, reducing the contaminants' portion to a deficient level (Sobolčiak et al., 2021). A recent study presented a PEG/MXene@MOF membrane with stable interlayer spacing and exceptional antifouling properties (Xiang et al., 2024a), demonstrating remarkable stability, high permeability, and an efficiency of 99.7% in purifying oil-in-water emulsions.

In the other study, a resilient PVA/GO@MOF membrane was tailored for efficient oil/water separation (Xiang et al., 2024b). This membrane showed superior self-cleaning properties, excels in resisting oil adhesion, maintains stable purification flux, and achieves high efficiency (>99.3%) in continuous crude oil emulsion purification.

As for the treatment of emulsified oil in water mixtures, droplets of colloidal dimensions (droplets' size below 500 nm) can be removed, which is not possible using the most common filtration method in an industry-based on walnut shell filtering media (Rahman, 1992; Yin et al., 2021; Dąbrowski, 2001; Sobolčiak et al., 2021; Sobolciak et al., 2020).

Recently, some new technologies for tertiary treatment utilizing absorption mechanisms have been developed and implemented. Edmiston et al. (2005); Burkett et al. (2008); Edmiston and Underwood (2009) developed the synthesis of highly oleophilic organosilicate gels based on organofunctional silanes. A novel type of these materials, Zerogels, instantaneously swell in unipolar organic solvents, increasing their volume more than three times. The swelling mechanism is reversible, making the materials suitable for repeated use after regeneration. The authors demonstrate these materials' applicability for water remediation, even if contaminated by dissolved organic pollutants (BETX compounds). ABS Materials produces these materials under the trademark Osorb® (Osorb® Media - ABS Materials, Inc, 2023). Other materials having the brand MYCELX RE-GEN and made by MYCELX Technologies Corporation (MYCELX REGEN, 2023) are based on the patents of H. Alper (Alper and Brooklyn, 1993, 1995) and were initially developed for the coagulation of free oils. Subsequently, it was adapted to design filtration media using porous media as carriers (paper, wood chips, vermiculite) to remove free oil and well emulsions with a droplet size of up to 2 (m). They are applicable for cleaning polluted waters up to 1000 ppm of oil inlet concentration and 5–50 ppm outlet (Produits coagulant le petrole et leurs procedes d'utilisation, 1996).

Furthermore, superhydrophobic sponges have showcased promising potential in oil/water separation. A study demonstrated a novel method employing amorphous carbon-coated polyurethane sponges to create superhydrophobic sponges, demonstrating exceptional oil absorption capacity (32–68 times the sponge weight) for diverse organic solvents and oils (Panickar et al., 2021). It highlights superior recyclability and efficiency for effective oil/water separation in turbulent conditions.

Another team prepared a highly hydrophobic and oleophilic sponge using a straightforward process, showcasing significant oil absorption capability for diverse oil spills and emulsified mixtures in static and turbulent water conditions (Khosravi and Azizian, 2015). The novelty of this study lies in the sponge's ability to retain structural integrity upon compression, enabling easy oil retrieval and its simple, cost-effective method for creating efficient sponges, ideal for oil spill cleanup and water filtration.

The present study showed the potential of novel the adsorbent prepared from recycled LDPE waste to purify emulsified oily polluted water in batch and filtration configurations. The separation efficiency of the novel adsorbent was tested in a filtration mode using deep-bed filtration technology, which is primarily applied in industry for the tertiary treatment of polluted waters. The comparison of the separation efficiency for various sorbents indicated a supreme performance of the adsorbent.

2. Experimental

2.1. Materials

Low-density polyethylene waste (LDPE – it will be denoted as "PE" in the whole text) was obtained from Qatar Petrochemical Company (QAPCO) in the form of pellets, ground in a high-energy mill, and sieved according to size. The fraction with an average size of 0.5 mm was selected and used for all the experiments. This choice was motivated by the utilization of sorbents in deep-bed filtration experiments. Particles with low dimensions decelerate a flow of liquids through the filtration column, thus increasing both the contact time and the pressure drop.

Synthetic-produced water was prepared according to the protocol developed by Dardor et al. (2021). using crude oil (Qatar Petroleum, Qatar), the salts (potassium chloride (KCl) (99%) (0.12 g/l), Sigma-Aldrich, sodium sulfate anhydrous (Na$_2$SO$_4$) (100%) (0.07 g/l), VWR chemicals, calcium chloride (CaCl$_2$) (90%) (0.84 g/l), ammonium chloride (NH$_4$Cl) (99.5–100.5%) (0.03 g/l), sodium chloride (NaCl) (99.5–100.5%) (2.39 g/l), magnesium chloride (MgCl$_2$) (95.21%) (0.24 g/l), BDH Chemicals Ltd Poole, and the surfactant sodium dodecyl sulfate (SDS; C$_{12}$H$_{25}$NaO$_4$S) (0.06 g/l), Riedel-de Haën. [3-(methacryloylamino)propyl]trimethylamonium chloride (MPTAC) was used as a 50% water solution and purchased from Sigma-Aldrich. The walnut shell was obtained from (Interactive Finishing Media, USA, size 12/20 grit), and the silica gel from (Riedel-de Haën, Germany).

2.2. Modification of PE powder

First, PE powder was sieved, and the 250–500 μm fraction was chosen for modification. The PE powder was treated by RF plasma (Plasma Etch Inc., Carson, CA, USA) in an air atmosphere with the power of 80 W and a time of 120 s to enhance the hydrophilicity of the PE surface. Then, 0.3 wt% of cationic monomer in ethanol was prepared and cast on PE powder in a petri dish at 3 g of PE to 10 ml of the monomer solution. Subsequently, the modified PE powder was dried in a vacuum at 60ºC. After drying, the PE powder was plasma treated under an Ar atmosphere at 80 W and for 120 s. After cleaning, this modified PE was washed extensively with distilled water until the TOC of the water contained below five ppm of TOC content.

2.3. Characterizations

The morphology of PE powders was characterized by a field emission scanning electron microscope (FE-SEM, Nova Nano SEM 650) combined with energy-dispersive X-ray spectroscopy (EDS).

X-ray photoelectron spectroscopy (XPS) was performed using a K Alpha + machine (Thermo, East Grinstead, UK) fitted with a monochromated X-ray source (1486.6 eV). The pass energy was set to 80 eV for the high-resolution spectra and 200 eV to acquire the survey regions. The surface static charge was compensated using a flood. The composition was determined using the manufacturer's sensitivity factors.

The size of oil droplets and zeta potential of emulsions were characterized by A Zetasizer Lab (Malvern Panalytical, UK). The total organic carbon (TOC) analysis was performed using a Formacs TOC/TN analyzer (Analytikjena, Germany).

2.4. The sorption tests

The sorption experiments were performed in the batch configuration using vial test tubes with a volume of 40 ml. The sorbent was inserted into vials filled with testing emulsions and closed. Sorption tests were realized over the selected periods at room temperature (22 °C) under stirring with a magnetic stirrer.

Column filtration tests were performed in a home-built testing unit capable of evaluating several media simultaneously under different loading conditions. The system consists of a positive displacement pump

(KNF, Switzerland) to control the flow through the columns (PFA, Swagelok, diameter: 0.95 cm) and pressure sensors to monitor the pressure increase as the columns get loaded with oil (Fig. 1). A pressure sensor (Omega Engineering, USA) was installed after each pump to record the operating pressure of each column. To avoid media floating, weighed amounts of glass wool (~45 mg) were added to the bottom and top of the column. The bed volume for all tested resins was set as ~10 ml (~14 cm as bed height). The flow of emulsion was 1 ml/min. Filtrates were periodically collected, and TOC was measured.

The saturated column was washed in situ using water, ethanol, and toluene. First, water was used to remove PW emulsion from a column, and then ethanol was used to remove water from the column. The next step was to use toluene, followed again by ethanol washing. The final step was extensive water washing to remove all ethanol from the column until the TOC of the water filtrate was under five ppm. The regenerated column was reused for the filtration of PW emulsion.

3. Results and discussion

3.1. Characterization of synthetic PW

The droplet size distribution within PW (carbon content of 120 ± 5 ppm) was determined from dynamic light scattering (DLS) measurements. The emulsion contained 63% of droplets with dimensions below 500 nm and 90% of droplets with sizes below 1000 nm, confirming the emulsion's colloidal character.

The zeta potential of PW was −54.0 mV, indicating the good kinetic stability of the emulsions.

3.2. Preparation and characterization of adsorbent

Fig. 2 shows the modification steps of PE powder by using a cationic MPTAC monomer. In the first step, PE powder is plasma treated in the air atmosphere, introducing hydroxyl, carboxyl, and peroxy groups on the surface of PE (Ghobeira et al., 2022). The next step, monomer deposition and drying, forms a thin monomer layer on the PE powders' surface. Finally, plasma treatment in an argon atmosphere was applied to the grafting and radical polymerization of the cationic MPTAC monomer (Kuzuya et al., 1986). The treated powder was washed in distilled water to remove unreacted monomers.

The SEM image of PE powder, modified by MPTAC with the average size of particles around 500 μm, is shown in Fig. 3a. EDS mapping of carbon, nitrogen, and oxygen distributed along the surface confirming modification of PE powder surface is shown in Fig. 3b. Fig. 3c, d show individual nitrogen and oxygen EDS mapping further confirming the homogenous surface modification.

Table 1 presents the XPS reports of the surface chemical composition of pristine and modified PE platforms. The various carbon, nitrogen, and oxygen species are deduced from the peak-fitted corresponding spectra. The total carbon content decreases from 98.2% to 91.4% and 90.9% for

Fig. 1. Filtration unit assembly.

plasma-treated PE, and the same surface after post-functionalization with a cationic polymer. Fig. 4a shows the surface oxidation of PE. In contrast, plasma treatment introduces more oxygen to the surface (see Table 1) as well as nitrogen species with a result of the appearance of a C-N - C1s component positioned at 285.7 eV shown in Table 1 and Fig. 4b. In addition, an increase in the surface proportion of C-OH O1s component can be seen from peak at 532.5 eV and presented in Table 1 and Fig. 4e-f. Both plasma and the cationic polymer introduce nitrogen-containing species as observed in the N1s region. The latter is fitted by two components positioned at 400.0 and 402.5 eV, assigned to C-N and C-N + species, respectively, in Fig. 4c-d. For the cationic polymer-post modified PE, the cationic polymer species implementation at the surface is proved by an increase in the N + /N atomic ratio from 0.43 to 0.65 and a remarkable increase in the signal-to-noise ratio, a sign of a second stage of PE modification essentially confined to the surface. Note that the pristine PE does not show any nitrogen atoms at the surface, as noted in the inset of Fig. 4c. Plasma treatment profoundly affects the surface oxygen content and corresponding O1s spectra. Table 1 shows a considerable increase in the atomic oxygen %, but a close look at the spectra indicates a higher count difference between the peak maximum and the baseline of about 45 kcps for PE Plasma (Fig. 4f), which is much higher than the 5.5 kcps for the neat PE surface (Fig. 4e).

XPS surface composition monitoring indicates significant chemical changes imparted by the plasma treatment and post-modification by cationic polymer deposition. This treatment creates an active polymeric layer, which promotes the adsorption of oil droplets on PE-based adsorbent. The separation mechanism is based on the attractive ion-ion electrostatic interaction among ammonium cations in poly[3-(methacryloylamino)propyl]trimethylamonium chloride layer, which was polymerized on PE surface, and sulfate anions originated by dissociation of sodium dodecyl sulfate surfactant, which was used for dispergation of crude oil in produced water. Further attractive electrostatic interactions such as ion-dipole and ion-induced dipole interactions may also enhance oil droplets' adsorption on a modified PE surface.

3.3. Sorption tests in the batch

3.3.1. Testing of adsorbent dosage

The effect of dosage on the separation performance of PW emulsions was investigated by varying the mass of sorbent from zero (blank experiment) to 1 g in a 40 ml vial. The concentration of carbon in the stock solution was 100 ± 3 ppm, and the experiment was conducted at 22 °C (RT) for 24 h, ensuring equilibrium had been reached. As indicated in Fig. 5, starting from 0.1 g, the further increase in dosage content only slightly increases the separation efficiency of the sorbent. Even though the separation efficiency of 0.1 g of the sorbent is the smallest one (except 0.05 g), considering the mass of adsorbed oil per mass of a sorbent (q_e) we get the highest values for that dosage value. For this reason, the dosage of 0.1 g was used in all further experiments. The losses during the experiment's running at the same conditions without sorbent were around 7 ± 3 ppm.

3.3.2. Testing of the initial oil concentration

The initial content of the oil phase in an emulsion influences the sorption capability of a sorbent because it results in a higher number of dispersed droplets and, therefore, more contact with the surface of sorbents. In this experiment, emulsions with different oil content were prepared, and the parameter q_e characterized the sorption capacities. Other conditions were kept constant.

The dependence $q_e = f(c_0)$, as shown in Fig. 6, is linear up to circa 150 ppm of initial oil content and then declines from linearity, indicating a deceleration of the adsorption uptake process, due to the approaching saturation of the accessible surface of the sorbent.

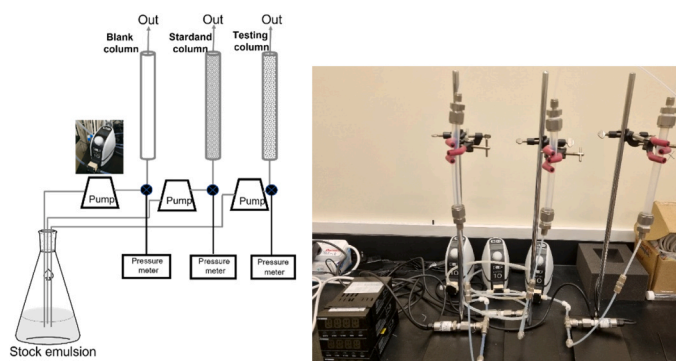The dependence of $q_e = f(c_0)$ in the region from) to 150 ppm can be expressed by a linear function (Eq.1):
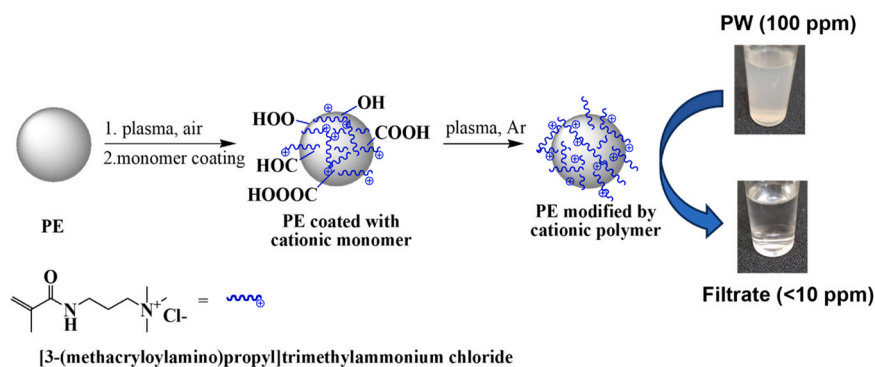
Fig. 2. The scheme of the modification of PE powder and formation of plasma treated (step 1) and poly(MPTAC) modified PE (step 2) that was used for produced water (PW) filtration (step 3).
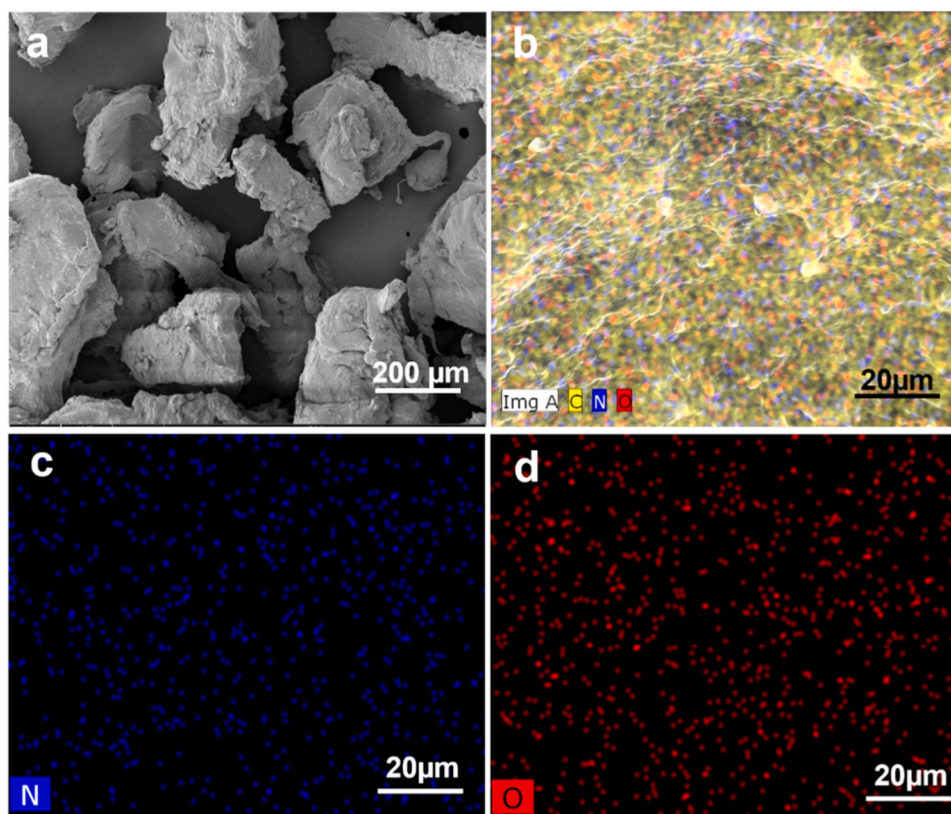

Fig. 3. a) SEM image, b) EDS-mapping, c) N element, and d) O element of cationic modified PE powder.

Table 1
Surface chemical composition of untreated and modified PE surfaces.

Sorbent	C_{285}	$C_{285.7}$	$C_{286.5}$	C_{288}	N_{400}	$N_{402.5}$	$O_{532.5}$	$O_{533.5}$	Cl
PE-neat	83.8		11.7	2.74	-	-	0.97	0.79	-
PE-plasma	73.3	10.4	4.95	2.73	0.23	0.10	6.62	1.63	-
PE-cationic	69.5	12.0	6.9	2.54	0.37	0.24	7.46	0.88	0.05

$$q_e = Kc_0 \qquad\qquad (1)$$

Where the parameter K= 0.2673 $\pm$ 0.00355 [kg/mg] (R^2 =0.99684).

3.3.3. Adsorption isotherms

Adsorption isotherms (AIs) are characterized by the dependence q_e = f(c_e). The mechanism of adsorption determines the shape of AIs. According to the shape, AIs are divided into six types (I-V) depending on their shape (Al-Ghouti and Da'ana, 2020). The dependence that is shown in Fig. 7 is S-shaped, which is typical for V-type isotherms (Wang and Guo, 2020; Foo and Hameed, 2010). This type of adsorption isotherm is observed if intermolecular attractive interactions are extensive and adsorption occurs in pores and capillaries (Al-Ghouti and Da'ana, 2020). The classical equilibrium isotherms, namely, the Langmuir and Freundlich isotherms, do not provide the best-fit correlations to oil uptake capacity data since the uptake of oil is often regarded as an
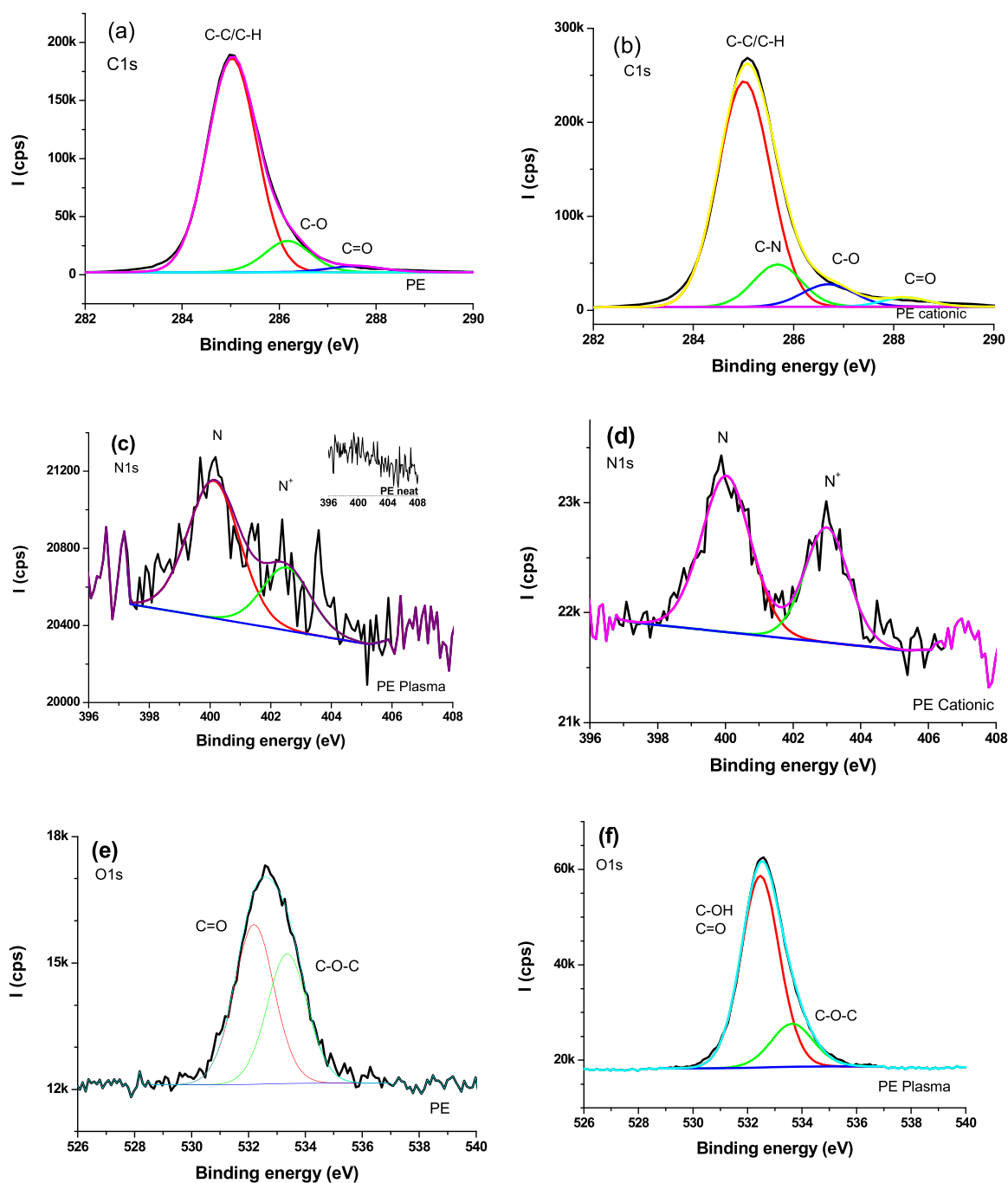
Fig. 4. High-resolution spectra of neat and modified PE. Peak-fitted C1s spectra of PE (a), and cationic polymer-modified PE (b); and N1s spectra of PE after plasma treatment (c) followed by cationic polymer deposition. O1s spectra are shown for PE (e), and plasma-treated PE (f).

absorption/adsorption process corresponding to several layers of ab/adsorbed oil. The Langmuir was developed for single-component, monolayer adsorption on a homogeneous eqi-energetic surface, which does not apply to oil uptake. The classical Freundlich model applies to a heterogeneous surface and can apply to single-component multilayer sorbate uptake. Based on the multilayer behavior of oil sorption and its multicomponent attributes, a modified Freundlich would seem appropriate for testing. This has been performed in the form of a Sips isotherm equation, which is discussed and tested.

The function f(x), which can describe the S-shape in general, has to have some basic mathematical features such as i) it increases with an increase in x (df/dx >0, it has an inflection point ($d^2f/dx^2 = 0$ in an inflection point), and iii.) it approaches a limit value for large x (x→∞).

A standard adsorption model that suits these conditions is the Sips isotherm model, expressed by Equation (2, a) (for liquids). The Sips isotherm (Sips, 1948) given by Eq. (2a) was initially developed for a description of gas adsorption on heterogeneous solid surfaces by a modification of Freundlich isotherm (Wang and Guo, 2020; Foo and Hameed, 2010; Freundlich, 1907).

This isotherm characterizes the distribution function of active sites on the sorbent's surface. Similarly to other isotherms, which were initially developed for the adsorption of gasses, the Sips isotherm was also adapted to describe solutes' adsorption from the liquid phase. The Sips isotherm can be simplified into Freundlich and Langmuir isotherm for low pressure (gases) of low solute concentrations.
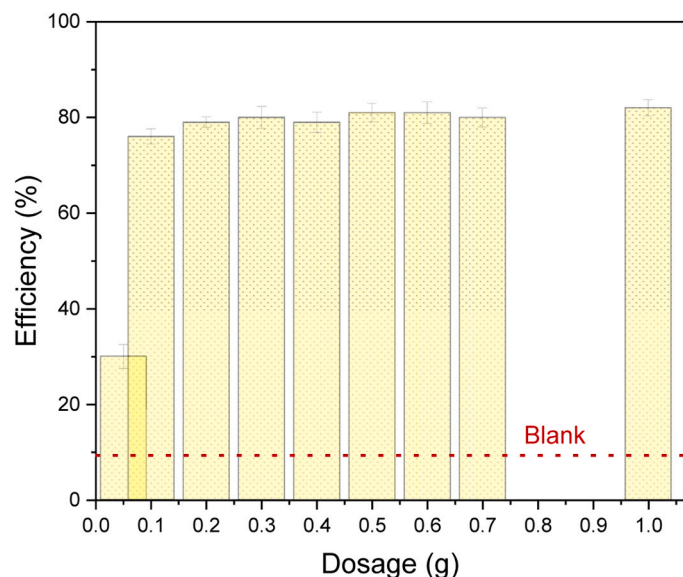
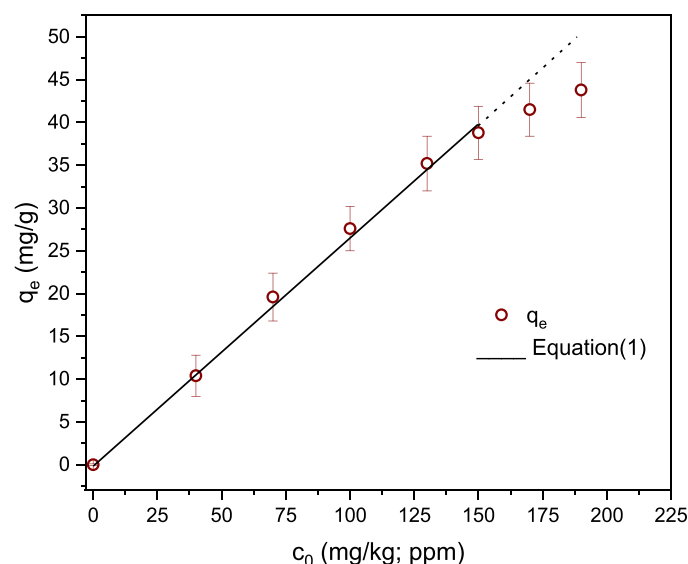**Fig. 5.** The removal efficiency for various dosages of the sorbent.

Fig. 7. The experimental dependence $q_e = f(c_e)$ (empty circles), and models given by Eq.(2a) (green solid), and Eq.(5a) (red dots).

Fig. 6. The dependence of q_e on the initial concentration of oil in emulsion (c_0).

$$q_e = \frac{q_m K_S c_e^n}{1 + K_S c_e^n} \tag{2a}$$

$$c_{e,i} = \left[\frac{n-1}{K_S(n+1)} \right]^{1/n} \tag{2b}$$

Where K_S is the Sips equilibrium constant [$(kg/mg)^{1/n}$], q_m [mg/g] is the maximum adsorption capacity, and n [-] is a fitting parameter. From Eq. (2b), it is clear that n must be >1, and also that n determines a position (a value) of the inflection point. Higher n results in a higher value of $c_{e,i}$.

The parameters obtained by fitting of the experimental data are q_m = 41.2 ± 1.4 [mg/g], K_S = (2.3 ± 0.5) x 10^{-5} [$(kg/mg)^{1/n}$], n = 3.5 ± 0.6, and $c_{e,i}$ = 18 ppm.

The applicability and limitations of the Sips isotherm were analyzed by De Vargas Brião et al. (2023).

The mathematically identical isotherm given by Eq. (2a) (Zhu and Gu, 1989; Gu and Zhu, 1990) was applied for a description of the adsorption of nonionic surfactants from aqueous solution onto polar adsorbents (e.g.,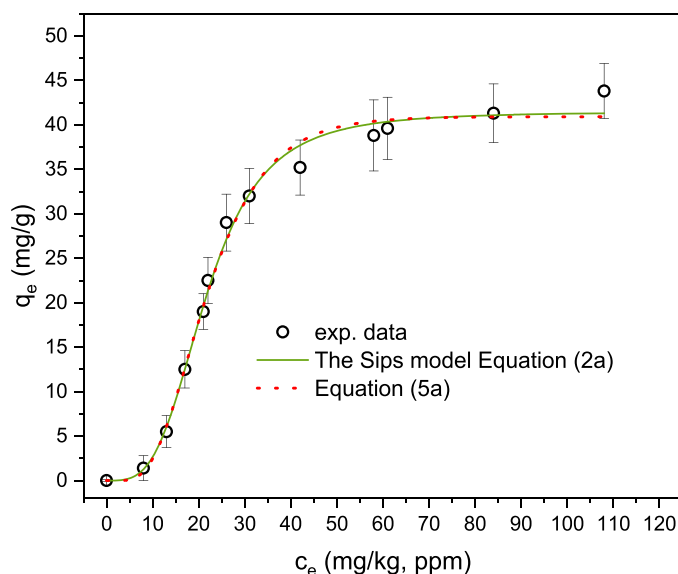 silica gel) using a mass-action model, and it is widely used for the characterization of surfactants' adsorption in general. In this model, the parameter n means the aggregation number of surface hydrophobic aggregates or hemi-micelles. The shape of sorption iso- therms and theoretical explanation of the parameter n in the Sips isotherm has been analyzed using statistical thermodynamic theory. Shimizu and Matubayasi, (2021) derived the cooperation isotherm without postulates concerning the adsorption sites, number of layers, pore size, and geometry. They stated that an isotherm's shape strongly depends on sorbent-sorbent interactions.

We refer to this model because of the uncommon S-shape of $q_e = f(c_e)$ dependence that was observed in this study. The experimental adsorp- tion isotherms and the related models describing the sorption of oil droplets from oil in water emulsions have mainly a convex trend upward (Type I isotherm) or a concave trend upward (Type III isotherm) shape (Albatrni et al., 2019; Al-Maas et al., 2022). The observed S-shape in this study may be associated with a surfactant attached to oil droplets. Therefore, the adsorption of droplets behaves similarly to the adsorption of pure surfactants. Indeed, the initial stage of the adsorption isotherm may be influenced by the adsorption of free, unbound surfactant that may be present in emulsions. The TOC determination does not enable the differentiation between carbon originating from crude oil species and carbon from surfactants. Therefore, an inspection of that hypothesis requires more sophisticated analytical techniques.

The Freundlich isotherm (Eq. (3)) is the most common isotherm that can describe dependences with both the convex and concave shape.

$$q_e = K_F c_e^m = K_F c_e^{\frac{1}{n}} \tag{3}$$

Where 1/n is the heterogeneity factor, n characterizes the intensity of the adsorption process and characterizes the relative distribution of the energy and the heterogeneity of the adsorbent reactive sites, and K_F [L/ mg] is the Freundlich adsorption constant.

Regardless of the actual physical meaning, the parameter m unam- biguously determines the shape of the Freundlich isotherm through Eq. (4).

$$\left(\frac{d^2 q_e}{dc_e^2} \right) = K_F m(m-1) c_e^{m-2} \tag{4}$$

If $m > 0$, then $\left(\frac{d^2 q_e}{dc_e^2} \right) > 0$ for the $m > 1$ (convex shape), and $\left(\frac{d^2 q_e}{dc_e^2} \right)$ < 0 for the $m < 1$ (concave shape). Many papers refer to the value m, or more frequently in the form of m= 1/n, as the parameter characterizing

favorable (m < 1) and unfavorable adsorption (m > 1). Despite the extensive use of this interpretation, it is not a generally accepted interpretation, missing a rigorous physical justification of this statement (Tran et al., 2017). However, regardless of the physical interpretation of the m, it differentiates the convex and concave shapes of the Freundlich isotherm. The evaluation of experimental data using Freundlich isotherm is shown in Figs. 8 and 9. Indeed, a single isotherm cannot be applied to fit the whole concentration region, and therefore, data were separated into two groups.

Figures show the applicability of Freundlich isotherm for c_e ≤ 25 ppm (Case I) and for c_e ≥ 25 ppm (Case II). This value was arbitrarily selected instead of $c_{e, i}$ = 18 ppm determined from Eq. (2b), as it better suits the separation of both regions and provides more accurate fits to the data. Then, for Case I we get K_F = 0.043 ± 0.04 [kg/mg], and n = 2.0 ± 0.3 (R^2 = 0.99684), and for Case II we get K_F = 75 ± 17 [kg/mg], and n = 0.24 ± 0.08 (R^2 = 0.97169). From these data, it is clear that Case I fits Case I much better than Case II; however, it is difficult to perform a deeper discussion of these values due to a lack of theoretical interpretation of those two parameters.

Complementary to the Sips' Equation, we have proposed a new empirical function given by Eq. (6a), which seems suitable for fitting experimental data.

$$q_e(c_e) = q_m[(1 - \exp(-kc_e)]^n \tag{5a}$$

$$c_{e,i} = \frac{\ln(n)}{k} \tag{5b}$$

q_m= 41 ± 2 [mg/g], k = 0.11 ± 0.02 [kg/mg], and n = 7 ± 2 [-] (R^2 =0.99679). The constant k can be formally defined as the adsorption equilibrium constant. Unlike the equilibrium constant provided by the Sips model, the dimensions of this constant do not depend on the parameter n. The inflection point Eq. (5b) was found from the second derivation of Eq. (5a), and it is $c_{e, i}$ = 18 [mg/kg; ppm]. This value corresponds to the initial concentration of around 67 ppm. It is the same value as determined by applying the Sips model. From this point, the shape of the adsorption isotherm changes from concave to convex. It is seen that this function gives an almost identical fit to the Sips model. The function can also be transferred to the Freundlich model at low c_e values, using a simple trick that the term $(1 - \exp(-kc_e)$ is expanded into the Taylor series, leading to the term kc_e, and after putting it into Eq.(5a) we get:
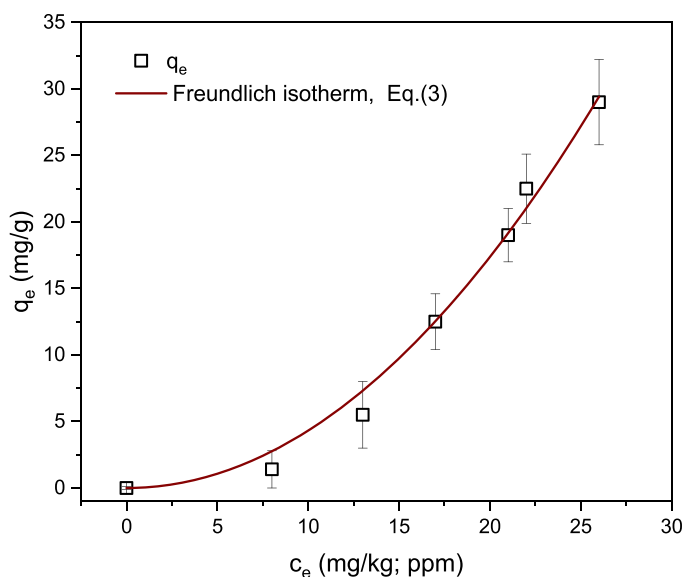

Fig. 8. The experimental dependence q_e =f(c_e) (squares), and the fit by Eq.(4) (red line) for the c_e ≤ 25 ppm.
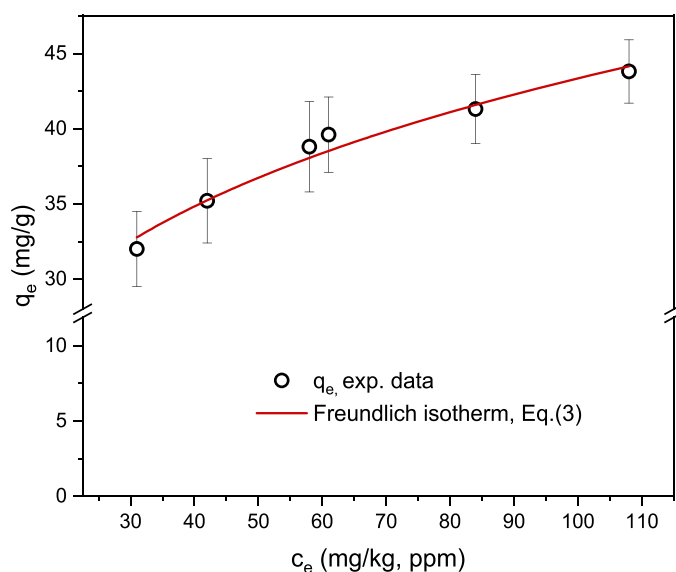

Fig. 9. The experimental dependence q_e =f(c_e) (circles), and the fit by Eq.(4) (red line) for the c_e ≥ 25 ppm.

$$q_e \approx (q_m k^n)c_e^n \equiv K_F c_e^n \tag{6}$$

3.3.4. The dependence of adsorption on temperature

In addition to experiments performed at 22 °C (RT), and referred to above, the adsorption was studied at higher temperatures 30, 40, 50, and 60 °C. The initial oil content was 40, 60, 80, and 100 ppm, the dosage was 0.1 g, and the duration of the experiments was 24 h. The TOC values were determined at the experiment's beginning and end and were used to calculate qe values. Unexpectedly, the q_e values did not change with an increased temperature observed and remained more or less the same constant value within a range of experimental error. Adsorption is an exothermic process (Dąbrowski, 2001), and therefore, in agreement with Le Chatelier's principle (Engel and Reid, 2024), the extent of adsorption usually decreases with an increase in temperature. Two speculative reasons would be provided to explain the observed discrepancy between an expectation and the experimental results. Firstly, physical adsorption is caused mainly by van der Waals interactions between permanent and induced dipoles, which inversely depend on temperature. Therefore, an increase in temperature has an unfavorable effect on adsorption (Dąbrowski, 2001). However, if the interaction between adsorbent and sorbate is based on Coulomb's forces between total charges, the temperature should not play a role since that one is temperature-independent. Secondly, an increase in temperature enhances the value of the diffusional coefficient of oil in water (D∝$D_0 e^{-1/T}$) (Engel and Reid, 2024), and therefore, the improved temperature can promote more contacts among oil droplets and sorbent's surface and act opposite to the common tendency.

3.3.5. Kinetics of adsorption

Kinetic models describe the time dependence of adsorption processes. In the batch systems, the solute concentration decreases until it reaches an equilibrium with adsorbed species. The concentration of a solute (c_e) is determined experimentally in selected periods, and the amount of adsorbate deposited on an adsorbent (q_t) is calculated. Unlike adsorption isotherms, only a few analytical models are commonly used to describe q_t =f(c_e) dependences. Three of the most frequently employed models are the pseudo-first-order kinetic model (PFOM) (Zur Theorie der sogenannten Adsorption gelöster Stoffe - Lagergreen, 1907), the pseudo-second-order kinetic model (PSOM) (Ho and McKay, 1998), and Weber-Morris intra-particle diffusion model (IPDM) (WeberJr.. and Morris, 1963), as shown in Fig.10. The models are expressed by
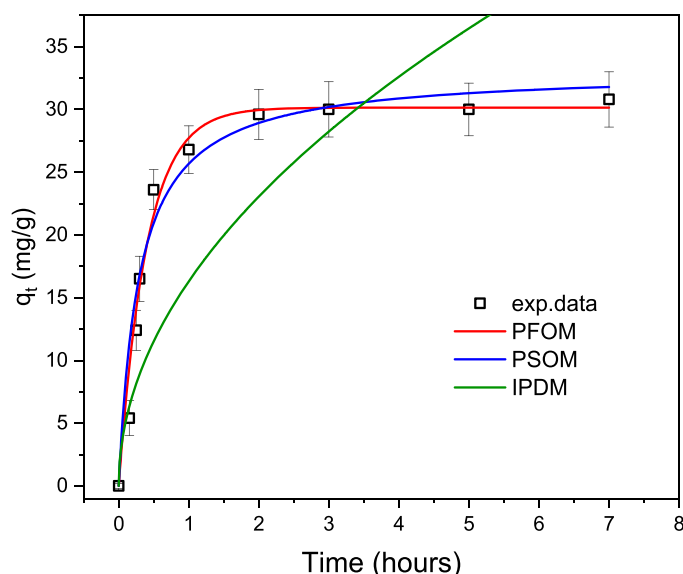
Fig. 10. The experimental dependence $q_t = f(t)$ (empty circles), PFOM (red solid line), PSOM (blue solid line), and IPDM (dotted green line).

non-linear Eq. (7) for PFOM, Eq. (8) for PSOM and Eq. (9) for IPDM. Each of these equations can be easily linearized; however, it has been preferred to use non-linear forms for fitting experimental data due to their higher accuracy (Revellame et al., 2020; Canzano et al., 2012).

$$q_t = q_e(1 - e^{(-k_1 t)}) \tag{7}$$

$$q_t = \frac{(k_2 q_e^2 t)}{(1 + k_2 q_e t)} \tag{8}$$

$$q_t = k_{ipd}\sqrt{t} + C \tag{9}$$

Where q_t is the amount of adsorbed species per mass of adsorbent [mg/g], k_1 [min^{-1}] is the pseudo-first-order rate constant, and k_2 is the pseudo-second-order rate constant mg/g.min], k_{ipd} [mg/g.min] is the rate constant for intra-particle diffusion, C [mg/g] is a constant related to the boundary layer thickness, and t is time [min].

q_e is an amount of adsorbed species per mass of adsorbent in equilibrium [mg/g], defined by Eq. (10):

$$q_e = \frac{(c_o - c_e)V}{m} \tag{10}$$

Where c_0 [mg/L] is an initial concentration, c_e [mg/L] is a concentration in equilibrium, V [L] is a volume of investigated liquid, and m [g] is a mass of the sorbent. The units mentioned here are the most common in literature, but different units can also be used.

It is seen that both PFOM and PSOM appropriately fit experimental data. IPDM is not convenient for the data description; however, it may not necessarily mean that diffusion plays no role in adsorption. As expressed by Eq. (9), the model describes only the Fickian type of diffusion, which may not be in line with diffusion into a porous PE sorbent with high pores' tortuosity. The parameters obtained from the fitting of experimental data by PFOM are $q_e = 30.4 \pm 0.9$ [mg/g], $k_1 = 2.3 \pm 0.2$ [h^{-1}], and R^2 = 0.99511, $q_e = 33.2 \pm 0.6$ [mg/g], $k_2 = 0.105 \pm 0.031$ [g/mg.h^{-1}], and R^2 = 0.99303 for fitting by PSOM.

3.4 Testing in the filtration mode (deep-bed filtration)

The sorption ability of the sorbent was tested in filtration mode at arbitrarily selected conditions. These conditions do not fully satisfy all conditions for deep bed filtration, for example, the length of the filtration column, and therefore, a typical breakthrough curve was observed

for no investigated sorbents. The target was comparing newly developed sorbents with common ones such as silica gel and walnut shells. Using this setup, the separation efficiency of the novel sorbent was around 65–70%, as shown in Fig.11. It is much higher than the separation efficiency of the industry's most commonly used medium (walnut shell). It is not a surprising observation due to the submicron (colloidal) character of PW used in this study. Walnut shell filters are efficient for emulsions having droplets size over 5 μm since the significant mechanism of oil removal is coalescence.

3.5 Cleaning and reuse of sorbents

The column filled with modified PE media was cleaned using water, ethanol, and toluene; subsequently, the column was extensively washed with distilled water. Among all the used washing agents, toluene is the most efficient solvent to clean columns from crude oil. However, due to the immiscibility of toluene with water in between steps, the additional use of ethanol has to be implemented.

The sorbent within the column was originally white, as seen in Fig.12a. Due to the sorption of the oil impurities, the sorbent in the column has turned brown. Fig.12b shows the column after PW filtration, where the sorbent's coloration within the column is caused by saturating the sorbent with crude oil from PW emulsion. Partial decoloration of the column caused by using ethanol and toluene has been observed. It is caused by removing the attached crude oil—(Fig.12c).

SEM/EDS analysis of sorbent after 1st filtration experiment and reused, cleaned media has been performed to confirm stability and presence of cationic monomeric unit on the surface of PE Fig.13. The size of particles in Fig.13a is similar to the size of sorbent of prepared cationic PE (Fig.13b). This confirms the structural stability and no abrasion of PE sorbent due to filtration and cleaning steps. Furthermore, EDS analysis demonstrates that the PE surface contains homogenously distributed O and N, which confirms stable and robust polymer modification on the surface of the PE sorbent.(Table 2).

After column cleaning, the same sorbent was reused to treat PW emulsion to compare fresh (1st) and PE media's separation efficiency. The separation efficiency decreased compared to 1st filtration, from 62 to 47% after five hours of filtration, as seen in Fig.14. The partial coloration of the column indicated some residual oil content of the cleaned column (Fig. 12c). However, even after extensive cleaning of the column, these residues were not being released from the column.
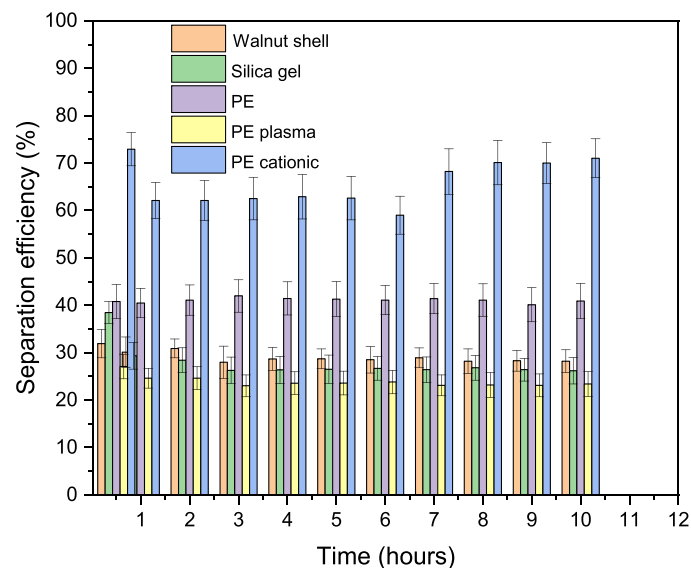

Fig. 11. Comparison of the separation efficiency of the selected sorbents in the filtration mode at the chosen arbitrary conditions.
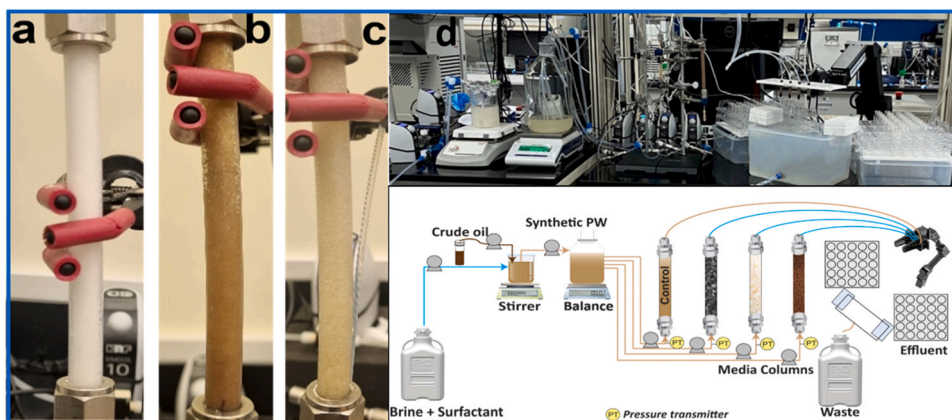
Fig. 12. Filtration column filled with modified PE after PW emulsion filtration a) before filtration, b) after 1st filtration, c) after the cleaning of PE media, d) the overall setup.
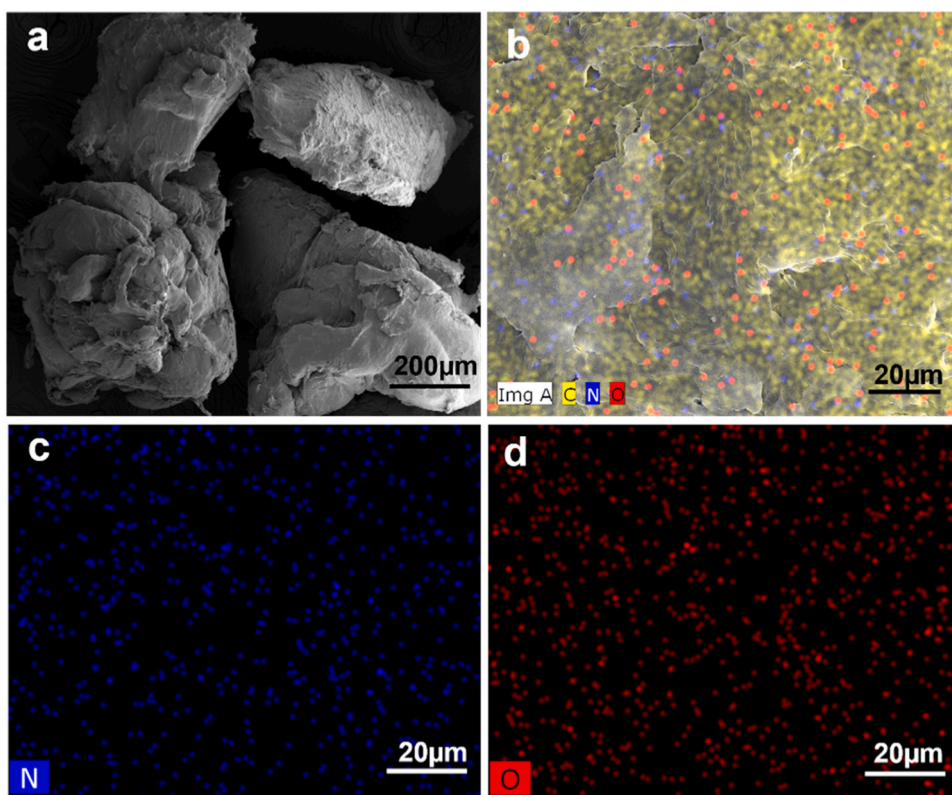

Fig. 13. a) SEM image, b) EDS-mapping, c) N element, and d) O element of used and cleaned cationic modified PE powder.

Table 2

Comparison of atomic percentage of C, O, and N elements on the surface of modified PE powder determined for prepared PE sorbent and after cleaning.

Element	EDS after modification (at%)	EDS after cleaning (at%)
C	94.2 (2.9)	94.0 (1.7)
O	2.3 (1.7)	2.1 (1.2)
N	3.5 (1.1)	3.8 (2.2)

4. Conclusions

This work has been motivated by the need to develop novel, alternative adsorbents for the purification of colloidal oily polluted waters originated by the petrochemical industry. The most commonly used technology based on walnut shell-based adsorbent does not enable the treatment of colloidal water and limits the oil droplet removal for sizes over 2–5 μm. Smaller species need to be separated by other methods, such as membrane filtration. On the other hand, the application of smart technologies, for instance, the sorbents based on organosilica gels or ion-exchanger-based resins, have a high price, which is not favorable for the purification of vast volumes of produced water coming from crude oil and gas extraction and processing.

This study prepared novel adsorbents designed from recycled low-density polyethylene (LDPE) powder grafted by cationic polymer. The cationic polymer was synthesized directly on the PE surface by plasma-induced radical polymerization, and this positively charged adsorbent showed a high affinity for negatively charged oil droplets. The efficient removal of crude oil contaminants from emulsified produced water (PW) was demonstrated. Synthetic PW was prepared to mimic actual PW
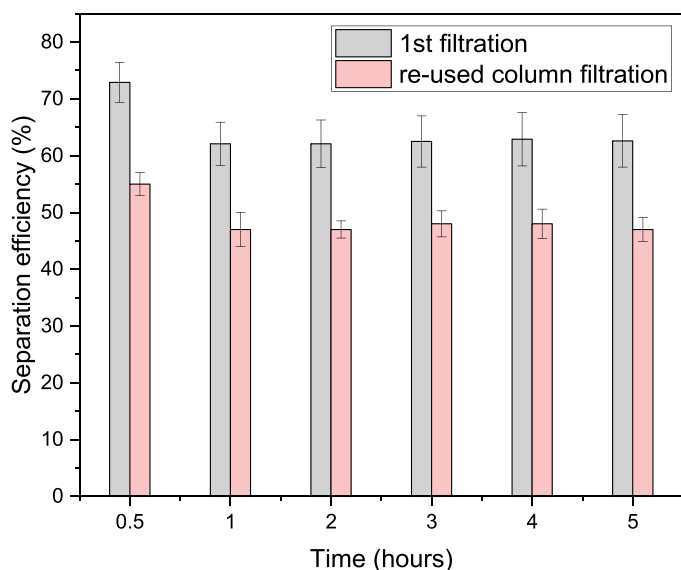
Fig. 14. Comparison of 1st and filtration after cleaning the sorbent within the column.

originating from the petrochemical industry. A detailed study of the adsorption isotherms and adsorption kinetics associated with the demulsification of PW in the batch has been performed. The adsorption isotherm showed a sigmoidal S-shape that was analyzed using the Sips isotherm and the new novel proposed empirical model. Both models produced an excellent correlation to the experimental data.

The separation efficiency of the novel adsorbent was also tested in a filtration mode mimicking a commonly used deep-bed filtration technology, which is mainly applied in industry for the tertiary treatment of polluted waters. The comparison of the separation efficiency for various sorbents indicated a supreme performance of our novel adsorbent against the reference materials. Indeed, this is only the ad-hoc comparison, valid for the arbitrarily chosen test conditions that cannot be extrapolated for large-scale designs.

This work demonstrated the ability of a relatively cheap adsorbent prepared from LDPE waste to purify emulsified oily, polluted water in batch and filtration configurations. This fact enhances the recycling possibilities of vast volumes of polyethylene waste, mainly low-density PE waste, with limited recycling potential.

Declaration of Competing Interest

The authors declare that they have no known competing financial interests or personal relationships that could have appeared to influence the work reported in this paper.

Acknowledgments

References

Adham, S., Hussain, A., Minier-Matar, J., Janson, A., Sharma, R., 2018. Membrane applications and opportunities for water management in the oil & gas industry. Desalination 440, 2–17. https://doi.org/10.1016/J.DESAL.2018.01.030.
Albatrni, H., Qiblawey, H., Almomani, F., Adham, S., Khraisheh, M., 2019. Polymeric adsorbents for oil removal from water. Chemosphere 233, 809–817. https://doi.org/10.1016/J.CHEMOSPHERE.2019.05.263.
Al-Ghouti, M.A., Da'ana, D.A., 2020. Guidelines for the use and interpretation of adsorption isotherm models: a review. J. Hazard Mater. 393, 122383 https://doi.org/10.1016/J.JHAZMAT.2020.122383.
Al-Ghouti, M.A., Al-Kaabi, M.A., Ashfaq, M.Y., Da'na, D.A., 2019. Produced water characteristics, treatment and reuse: a review. J. Water Process Eng. 28, 222–239. https://doi.org/10.1016/J.JWPE.2019.02.001.
Al-Kaabi, M.A., Al-Ghouti, M.A., Ashfaq, M.Y.M., Ahmed, T., Zouari, N., 2019. An integrated approach for produced water treatment using microemulsions modified activated carbon. J. Water Process Eng. 31, 100830 https://doi.org/10.1016/J.JWPE.2019.100830.
Al-Maas, M., Minier-Matar, J., Krupa, I., Al-Maadeed, M.A.A., Adham, S., 2022. Evaluation of polymeric adsorbents via fixed-bed columns for emulsified oil removal from industrial wastewater. JWPE 49, 102962. https://doi.org/10.1016/J.JWPE.2022.102962.
Alper, H., Brooklyn, N.Y., 1993, Coagulant for Oil Glyceride/isobutyl Methacrylate Composition and Method of Use.
Alper, H., Brooklyn, N.Y., 1995, Composition for Coagulating Oil.
Burkett, C.M., Edmiston, P.L., 2005. Highly swellable sol–gels prepared by chemical modification of silanol groups prior to drying. J. Non Cryst. Solids 351, 3174–3178. https://doi.org/10.1016/J.JNONCRYSOL.2005.08.015.
Burkett, C.M., Underwood, L.A., Volzer, R.S., Baughman, J.A., Edmiston, P.L., 2008. Organic-inorganic hybrid materials that rapidly swell in non-polar liquids: nanoscale morphology and swelling mechanism. Chem. Mater. 20, 1312–1321. https://doi.org/10.1021/CM0716001/SUPPL_FILE/CM0716001-FILE002.PDF.
Canzano, S., Iovino, P., Leone, V., Salvestrini, S., Capasso, S., 2012. Use and misuse of sorption kinetic data: a common mistake that should be avoided. Adsorp. Sci. Techno 30, 217–225. https://doi.org/10.1260/0263-6174.30.3.217.
Dąbrowski, A., 2001. Adsorption — from theory to practice. Adv. Colloid Interface Sci. 93, 135–224. https://doi.org/10.1016/S0001-8686(00)00082-8.
Dardor, D., Al-Maas, M., Minier-Matar, J., Janson, A., Sharma, R., Hassan, M.K., Al-Maadeed, M.A.A., Adham, S., 2021. Protocol for preparing synthetic solutions mimicking produced water from oil and gas operations. ACS Omega 6, 6881–6892. https://doi.org/10.1021/ACSOMEGA.0C06065/ASSET/IMAGES/LARGE/AO0C06065_0012.JPEG.
De Vargas Brião, G., Ali, M., Khim, H., Chu, H., Hashim, A., Chu, K.H., 2023. The Sips isotherm equation: often used and sometimes misused. Sep. Sci. Technol. 58, 884–892. https://doi.org/10.1080/01496395.2023.2167662.
Dickhout, J.M., Moreno, J., Biesheuvel, P.M., Boels, L., Lammertink, R.G.H., de Vos, W.M., 2017. Produced water treatment by membranes: a review from a colloidal perspective. J. Colloid Interface Sci. 487, 523–534. https://doi.org/10.1016/J.JCIS.2016.10.013.
Dores, R., Hussain, A., Katebah, M., Adham S., 2012, Using Advanced Water Treatment Technologies To Treat Produced Water From The Petroleum Industry, SPE Production and Operations Symposium, https://doi.org/10.2118/157108-MS.
Edmiston, P.L., Underwood, L.A., 2009. Absorption of dissolved organic species from water using organically modified silica that swells. Sep Purif. Technol. 66, 532–540. https://doi.org/10.1016/J.SEPPUR.2009.02.001.
Engel, T., (Philip J.) Reid, P., 2024, Thermodynamics, Statistical Thermodynamics, and Kinetics, (n.d.) 656.
Foo, K.Y., Hameed, B.H., 2010. Insights into the modeling of adsorption isotherm systems. J. Chem. Eng. 156, 2–10. https://doi.org/10.1016/J.CEJ.2009.09.013.
Freundlich, H., 1907. Über die Adsorption in Lösungen. Z. Phys. Chem. 57U, 385–470. https://doi.org/10.1515/ZPCH-1907-5723.
Ghobeira, R., Esbah Tabaei, P.S., Morent, R., De Geyter, N., 2022. Chemical characterization of plasma-activated polymeric surfaces via XPS analyses: a review. Surf. Interfaces 31, 102087. https://doi.org/10.1016/J.SURFIN.2022.102087.
Gu, T., Zhu, B.Y., 1990. The S-type isotherm equation for adsorption of nonionic surfactants at the silica gel—water interface. Colloids Surf. 44, 81–87. https://doi.org/10.1016/0166-6622(90)80189-B.
Ho, Y.S., McKay, G., 1998. The kinetics of sorption of basic dyes from aqueous solution by sphagnum moss peat. Can. J. Chem. Eng. 76, 822–827. https://doi.org/10.1002/CJCE.5450760419.
Igunnu, E.T., Chen, G.Z., 2014. Produced water treatment technologies. Int. J. Low Carbon Technol. 9, 157–177. https://doi.org/10.1093/IJLCT/CTS049.
Industrial Wastewater Treatment Technology, Second edition (Book) | OSTI.GOV, (n.d.). ⟨https://www.osti.gov/biblio/7253209⟩ (Accessed June 11, 2023).
Khosravi, M., Azizian, S., 2015. Synthesis of a novel highly oleophilic and highly hydrophobic sponge for rapid oil spill cleanup. ACS Appl. Mater. Interfaces 7, 25326–25333. https://doi.org/10.1021/ACSAMI.5B07504/SUPPL_FILE/AM5B07504_SI_002.ZIP.
Kuzuya, M., Kawaguchi, T., Yanagihara, Y., Nakai, S., Okuda, T., 1986. Mechanism of plasma-initiated polymerization: concerning the nature of solvent effects on the lifelike polymerization of water-soluble vinyl monomers. J. Polym. Sci. A Polym. Chem. 24, 707–713. https://doi.org/10.1002/POLA.1986.080240414.
Munirasu, S., Haija, M.A., Banat, F., 2016. Use of membrane technology for oil field and refinery produced water treatment—a review. Process Saf. Environ. Prot. 100, 183–202. https://doi.org/10.1016/J.PSEP.2016.01.010.

MYCELX REGEN, (n.d.). ⟨https://mycelx.com/technologies/mycelx-regen/⟩ (Accessed June 11, 2023).

Neff, J., Lee, K., DeBlois, E.M., 2011. Produced water: overview of composition, fates, and effects. Prod. Water 3–54. https://doi.org/10.1007/978-1-4614-0046-2_1.

Osorb® Media - ABS Materials, Inc. Advanced Material Solutions, (n.d.). ⟨https://sites.google.com/a/absmaterials.com/mockup/osorbmedia⟩ (Accessed June 11, 2023).

Padaki, M., Surya Murali, R., Abdullah, M.S., Misdan, N., Moslehyani, A., Kassim, M.A., Hilal, N., Ismail, A.F., 2015. Membrane technology enhancement in oil–water separation. a review. Desalination 357, 197–207. https://doi.org/10.1016/J.DESAL.2014.11.023.

Panickar, R., Sobhan, C.B., Chakravorti, S., 2021. Highly efficient amorphous carbon sphere-based superhydrophobic and superoleophilic sponges for oil/water separation. Langmuir 37, 12501–12511. https://doi.org/10.1021/ACS.LANGMUIR.1C02307.

Pintor, A.M.A., Vilar, V.J.P., Botelho, C.M.S., Boaventura, R.A.R., 2016. Oil and grease removal from wastewaters: sorption treatment as an alternative to state-of-the-art technologies. A critical review. Chem. Eng. J. 297, 229–255. https://doi.org/10.1016/J.CEJ.2016.03.121.

Produits Coagulant Le Petrole Et Leurs Procedes D'utilisation, 1996.

Rahman, S.S., 1992. Evaluation of filtering efficiency of walnut granules as deep-bed filter media. J. Pet. Sci. Eng. 7, 239–246. https://doi.org/10.1016/0920-4105(92)90021-R.

Revellame, E.D., Fortela, D.L., Sharp, W., Hernandez, R., Zappi, M.E., 2020. Adsorption kinetic modeling using pseudo-first order and pseudo-second order rate laws: a review. Clean. Eng. Technol. 1, 100032 https://doi.org/10.1016/J.CLET.2020.100032.

Shimizu, S., Matubayasi, N., 2021. Cooperative sorption on porous materials. Langmuir 37, 10279–10290. https://doi.org/10.1021/ACS.LANGMUIR.1C01236/ASSET/IMAGES/MEDIUM/LA1C01236_M059.GIF.

Sips, R., 1948. On the structure of a catalyst surface. J. Chem. Phys. 16, 490–495. https://doi.org/10.1063/1.1746922.

Sobolciak, P., Popelka, A., Tanvir, A., Al-Maadeed, M.A., Adham, S., Krupa, I., 2020. Materials and technologies for the tertiary treatment of produced water contaminated by oil impurities through nonfibrous deep-bed media: a review. , 3419 Water Vol. 12 (12), 3419. https://doi.org/10.3390/W12123419.

Sobolčiak, P., Popelka, A., Tanvir, A., Al-Maadeed, M.A., Adham, S., Krupa, I., 2021. Some theoretical aspects of tertiary treatment of water/oil emulsions by adsorption and coalescence mechanisms: a review. , 652. 13 Water Vol. 13, 652. https://doi.org/10.3390/W13050652.

Tanudjaja, H.J., Hejase, C.A., Tarabara, V.V., Fane, A.G., Chew, J.W., 2019. Membrane-based separation for oily wastewater: a practical perspective. Water Res. 156, 347–365. https://doi.org/10.1016/J.WATRES.2019.03.021.

Tran, H.N., You, S.J., Hosseini-Bandegharaei, A., Chao, H.P., 2017. Mistakes and inconsistencies regarding adsorption of contaminants from aqueous solutions: a critical review. Water Res. 120, 88–116. https://doi.org/10.1016/J.WATRES.2017.04.014.

Wang, J., Guo, X., 2020. Adsorption isotherm models: classification, physical meaning, application and solving method. Chemosphere 258, 127279. https://doi.org/10.1016/J.CHEMOSPHERE.2020.127279.

WeberJr, W.J., Morris, J.C., 1963. Kinetics of adsorption on carbon from solution. J. Sanit. Eng. Div. 89, 31–59. https://doi.org/10.1061/JSEDAI.0000430.

Xiang, B., Gong, J., Sun, Y., Yan, W., Jin, R., Li, J., 2024a. High permeability PEG/MXene@MOF membrane with stable interlayer spacing and efficient fouling resistance for continuous oily wastewater purification. J. Memb. Sci. 691, 122247 https://doi.org/10.1016/J.MEMSCI.2023.122247.

Xiang, B., Gong, J., Sun, Y., Li, J., 2024b. Robust PVA/GO@MOF membrane with fast photothermal self-cleaning property for oily wastewater purification. J. Hazard. Mater. 462, 132803 https://doi.org/10.1016/J.JHAZMAT.2023.132803.

Yin, X., Zhang, J., Wang, X., Zhu, M., 2021. Modified walnut shell filter material for the enhanced removal of oil from oilfield wastewater. Environ. Eng. Res. 26 (1), 6. https://doi.org/10.4491/EER.2019.369.

Zhu, B.Y., Gu, T., 1989. General isotherm equation for adsorption of surfactants at solid/liquid interfaces. Part 1. Theoretical. J. Chem. Soc. Faraday Trans. 1 Phys. Chem. Condens. Ph. 85, 3813–3817. https://doi.org/10.1039/F19898503813.

Zur Theorie der sogenannten Adsorption gelöster Stoffe - Lagergreen, S., (Bihang A. K. Svenske Vet. Ak. Handl. 24, II. Nr. 4, S. 49; 1899; Z. physik. Ch. 32, 174–75; 1900.), Zeitschrift Für Chemie Und Industrie Der Kolloide. 2 (1907) 15. https://doi.org/10.1007/BF01501332/METRICS.